Data analysis techniques for stereo IACT systems

Werner Hofmann, for the HEGRA collaboration

Max-Planck-Institut für Kernphysik, P.O. Box 103980, D-69029 Heidelberg, Germany

Abstract. Based on data and Monte-Carlo simulations of the HEGRA IACT system, improved analysis techniques were developed for the determination of the shower geometry and shower energy from the multiple Cherenkov images. These techniques allow, e.g., to select subsamples of events with better than 3' angular resolution, which are used to limit the rms radius of the VHE emission region of the Crab Nebula to less than 1.5'. For gamma-rays of the Mrk 501 data sample, the energy can be determined to typically 10% and the core location to 2-3 m.

Systems of imaging atmospheric Cherenkov telescopes (IACTs) for TeV gamma-ray astronomy allow the stereoscopic reconstruction of air showers, and provide improved angular resolution, energy resolution, and rejection of backgrounds such as showers induced by cosmic rays, local muons, or random triggers caused by night-sky background light. For systems with more than two telescopes, the shower parameters are overdetermined, allowing important cross-checks of the performance of the telescope system and of the reconstruction algorithms. In particular, the event-by-event determination of the position of the core permits to directly measure effective detection areas, and to estimate the systematic errors in the flux measurement [1,2].

In this talk, I will cover recent developments concerning improved algorithms to reconstruct shower direction and shower energy, and their tests using data from the HEGRA IACT system [3,2]. Detailed information as well as a more complete list of references can be found in [4–6].

Reconstruction of the shower geometry [4]. The traditional reconstruction algorithm used in HEGRA determines the shower direction by intersecting the axes of all Cherenkov images, regardless of the quality of individual images (Fig. 1(a)). In particular in events combining some bright images with dim images, the latter, with their poorly determined image parameters, can spoil the angular resolution. The angular resolution can be improved by estimating, for each image, the errors on the image parameters and by properly propagating these errors (Fig. 1(b)). In addition, one can use the shape of the image, in particular the *width/length* ratio, to estimate the *distance d* between the image centroid and the source, and use this information to derive, for each telescope, an error ellipse for the source location (actually, two ellipses, because of the head-tail ambiguity). The ellipses from different telescopes are then combined to locate the source (Fig. 1(c)). Finally, another approach (d) is to fit the intensity distribution of the images using a set of image templates, rather than parameterizing images by their Hillas parameters. Fig. 1(e) shows the angular resolution for achieved for different event classes. As expected, the techniques (b)-(d) outperform the simplest algorithm (a). The fit (d) is generally best, but the improvement compared to the much simpler and faster algorithm (c) is not dramatic. In addition to an improvement in the angular resolution, algorithms (b)-(d) provide, for each event, an estimate of the angular resolution (Fig. 2(a)), which can be used, e.g., to reject poorly reconstructed events.

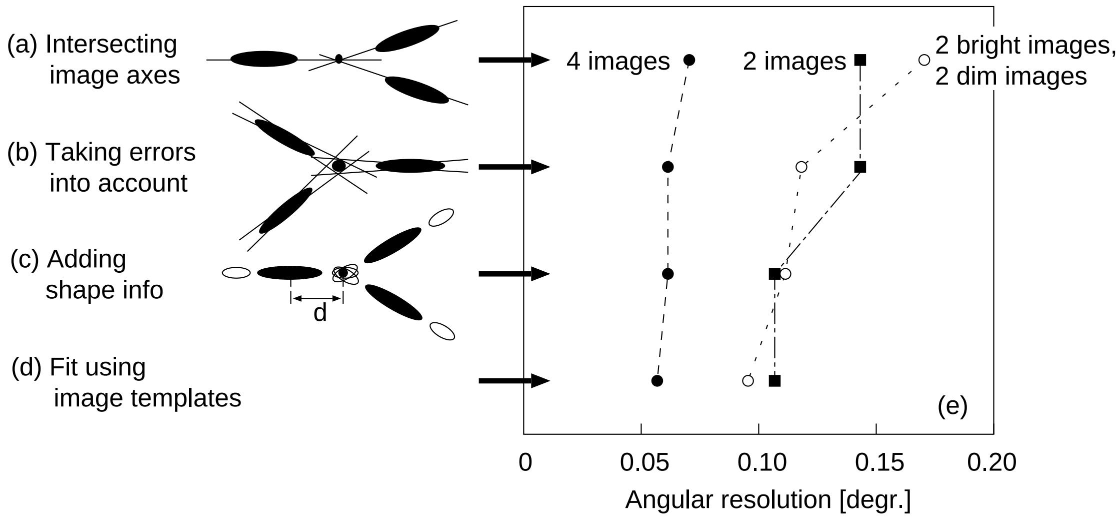

FIGURE 1. (left) Illustration of different algorithms to reconstruct the shower direction from the multiple Cherenkov images. (right) Resulting mean angular resolution for different data sets.

Size of VHE emission region of the Crab Nebula [6]. Well-reconstructed events reach an angular resolution on the same scale as the characteristic size of the Crab Nebula. One can use such events to search for evidence for an extended VHE emission region. Fig. 2(b) shows the angular distribution of events with an estimated angular error of less than 3' in each projection, relative to the direction to the Crab. The width of the distribution is, within statistical errors, identical with the width expected for a point source on the basis of simulations (Fig. 2(c)) and with the width of the gamma-ray distribution observed for Mrk 501. Therefore, we can only give an upper limit on the size of the emission region. Including systematic effects, e.g. due to pointing errors, we find a 99% upper limit on the rms radius $< r^2 >$ of the TeV emission region of 1.5'. This value is comparable to the radius at radio wavelengths, but significantly larger than the size at x-ray energies. Standard models for the VHE gamma-ray emission of the Crab Nebula assume that the same electron population is responsible for x-rays via synchrotron emission, and for TeV gamma-rays via the IC process, and predict a small TeV emission region, well below the experimental limit. Possible hadronic production of gamma-rays, on the other hand, could take place at significantly larger distances from the pulsar.

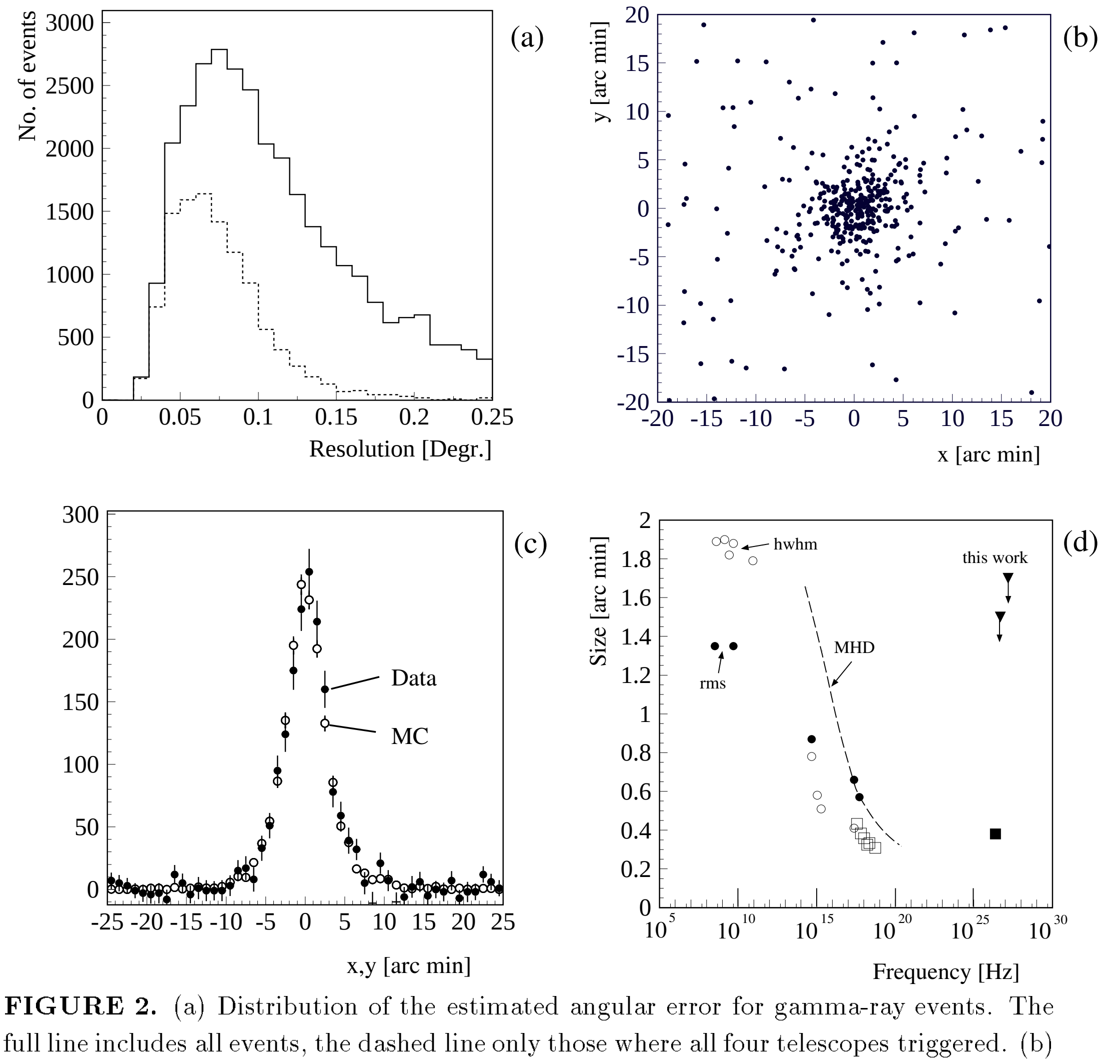

FIGURE 2. (a) Distribution of the estimated angular error for gamma-ray events. The full line includes all events, the dashed line only those where all four telescopes triggered. (b) Angular distribution relative to the direction to the Crab pulsar, for gamma-rays with estimated reconstruction errors of less than 3' in each direction. (c) Distribution of gamma-ray directions, compared to Monte-Carlo simulations assuming a point source. (d) Rms radius of the photon emission region in the Crab nebula, as a function of frequency, including the upper limits obtained at TeV energies.

Core determination [5]. The shower core is usually located by intersecting the image axes, starting from the telescope locations. The precision of the core determination is therefore given by the precision with which the image axes can be determined, typically $O(5^\circ)$. If the source location is known, as is the case, e.g., for the Mrk 501 data sample, one can alternatively determine the image axis as the line connecting the image of the source and the image centroid. With a typical distance between the source and the image centroid of 1° and a measurement of the centroid to $O(0.02^\circ)$, the image axis is then known to $O(1^\circ)$. Using this technique, Monte Carlo simulations predict that the precision for the shower core improves from about 6 m to 10 m for the normal method, to about 2 m to 3 m, depending on the core distance (in each case, properly taking into account the errors on the measured image parameters). The exact knowledge of the core position is particularly important for the energy determination, when the observed light yield is translated into an energy estimate.

Energy determination [5]. Earlier studies comparing event-by-event the light yield observed in different telescopes indicated correlated fluctuations in the light yield of individual showers [1]. Monte-Carlo studies point to the fluctuation in the height of the shower maximum as the primary source for these correlated fluctuations. Fig. 3(a) illustrates that for distances up to about 100 m from the shower axis, the light yield varies significantly with the height of the shower; only beyond the Cherenkov radius of about 120 m is the light yield stable. An obvious approach to improve the energy resolution is therefore to measure the height h_{max} of the shower maximum, and to include it as an additional parameter, writing $E_i = f(size_i, r_i, h_{max})$, where $size_i$ is the image *size* measured in telescope i at a distance r_i from the shower axis. With an IACT system, the height of the shower maximum, or, more precisely, the height of maximum Cherenkov emission, can be determined essentially by triangulation, using the relation between the *distance* d_i from the image to the source, r_i, and h_{max}: $d_i \approx r_i/h_{max}$. The actual algorithm [5] uses a slightly more complicated relation, reflecting the fact that light arriving at small r_i is generated by the tail of the shower rather than by particles near the shower maximum. The algorithm reaches a resolution in shower height of 530 to 600 m rms.

Fig. 3(b) illustrates the effect of the various possible improvements to the energy resolution. Whereas the conventional algorithm provides a resolution of 18% to 22% for the 1 TeV to 30 TeV range, the shower-height correction provides a resolution of about 12% to 14%, and the combination of the shower height correction with the improved core determination assuming a known source yields 9% to 12% resolution.

Before applying this technique to the actual data to obtain improved energy spectra, one needs to make sure that systematic effects are under control at a level consistent with the improved resolution. While the redundant data from the IACT system provide sufficient information to check this, the analysis is not yet finished. A first test of the new method with Mrk 501 data results in a spectrum consistent with earlier analyses, possibly with a slightly steeper spectrum in the cutoff region beyond 6 TeV.

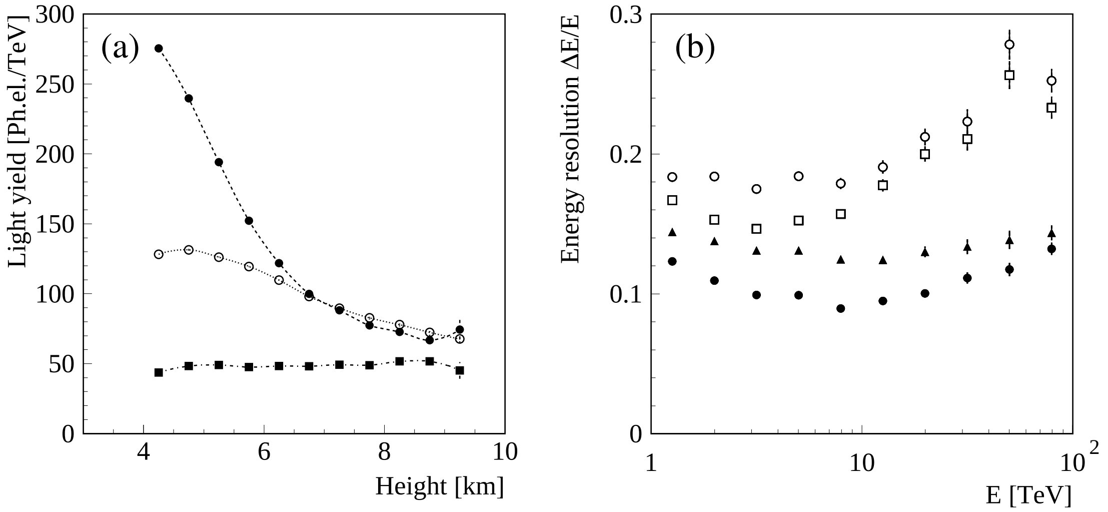

FIGURE 3. (a) Light yield (in Photoelectrons/TeV) as a function of the height of maximum Cherenkov emission, at core distances around 40-50 m (full circles), 90-100 m (open circles) and 140-150 m (full squares). (b) Energy resolution as a function of energy, for the conventional energy reconstruction (open circles), with improved core determination (open squares), with shower height correction (full triangles), and with shower height correction and improved core determination (full circles).

Summary. The analysis algorithms discussed here represent clear improvements over the first-generation algorithms used in the reconstruction of data from the HEGRA IACT system; it is also clear that further improvements are possible and that at this point we do not fully use all the information provided by multiple IACT images of an air shower. The algorithms do not only improve the angular resolution and the energy resolution; they also help to boost the significance of faint signals. For example, instead of simply counting all events reconstructed within a certain angular distance form a source, one can form a weighted sum, weighting events according to their expected signal-to-background ratio, as determined event-by-event from the estimated angular error and misidentification probability. First tests of such methods indicate in an increase in the significance for the detection of weak sources by up to 80%.

Acknowledgments. Many of the members of the MPIK CT group have contributed in one way or another to the development and tests of the advanced analysis techniques discussed here; in particular, I. Jung, A. Konopelko, H. Lampeitl, H. Krawczynski and G. Pühlhofer should be mentioned.

REFERENCES

1. W. Hofmann, Proceedings of the Int. Workshop "Towards a Major Atmospheric Cherenkov Detector V", Kruger Park, (1997), p. 284, and astro-ph/9710297 (1997).
2. F.A. Aharonian et al., Astron. Astrophys. 342 (1999) 69, 349 (1999) 11.
3. A. Daum et al., Astroparticle Phys. 8 (1997) 1.
4. W. Hofmann et al., Astroparticle Phys., in press, and astro-ph/9904234.
5. W. Hofmann et al., Astroparticle Phys., in press, and astro-ph/9908092.
6. F.A. Aharonian et al., in preparation.